

Article

Removal of Barium, Cobalt, Strontium, and Zinc from Solution by Natural and Synthetic Allophane Adsorbents

Andre Baldermann ^{1,*} , Andrea Căcilia Griessbacher ¹, Claudia Baldermann ², Bettina Purgstaller ¹, Ilse Letofsky-Papst ³, Stephan Kaufhold ⁴ and Martin Dietzel ¹ 

¹ Institute of Applied Geosciences, Graz University of Technology, Rechbauerstraße 12, 8010 Graz, Austria; andrea.griessbacher@student.tugraz.at (A.C.G.); bettina.purgstaller@tugraz.at (B.P.); martin.dietzel@tugraz.at (M.D.)

² Institute of Technology and Testing of Building Materials, Graz University of Technology, Inffeldgasse 24, 8010 Graz, Austria; claudia.baldermann@tugraz.at

³ Institute for Electron Microscopy and Nanoanalysis and Center for Electron Microscopy, Graz University of Technology, Steyrergasse 17, 8010 Graz, Austria; ilse.papst@felmi-zfe.at

⁴ BGR, Bundesanstalt für Geowissenschaften und Rohstoffe, Geozentrum Hannover, Stilleweg 2, 30655 Hannover, Germany; stephan.kaufhold@bgr.de

* Correspondence: baldermann@tugraz.at; Tel.: +43-(0)316-873-6850

Received: 28 June 2018; Accepted: 17 August 2018; Published: 21 August 2018



Abstract: The capacity and mechanism of the adsorption of aqueous barium (Ba), cobalt (Co), strontium (Sr), and zinc (Zn) by Ecuadorian (NatAllo) and synthetic (SynAllo-1 and SynAllo-2) allophanes were studied as a function of contact time, pH, and metal ion concentration using kinetic and equilibrium experiments. The mineralogy, nano-structure, and chemical composition of the allophanes were characterized by X-ray diffraction, Fourier transform infrared spectroscopy, transmission electron microscopy, and specific surface area analyses. The evolution of adsorption fitted to a pseudo-first-order reaction kinetics, where equilibrium between aqueous metal ions and allophane was reached within <10 min. The metal ion removal efficiencies varied from 0.7 to 99.7% at pH 4.0 to 8.5. At equilibrium, the adsorption behavior is better described by the Langmuir model than by the Dubinin–Radushkevich model, yielding sorption capacities of 10.6, 17.2, and 38.6 mg/g for Ba²⁺, 12.4, 19.3, and 29.0 mg/g for HCoO₂⁻; 7.2, 15.9, and 34.4 mg/g for Sr²⁺; and 20.9, 26.9, and 36.9 mg/g for Zn²⁺, by NatAllo, SynAllo-2, and SynAllo-1, respectively. The uptake mechanism is based on a physical adsorption process rather than chemical ion exchange. Allophane holds great potential to effectively remove aqueous metal ions over a wide pH range and could be used instead of other commercially available sorbent materials such as zeolites, montmorillonite, carbonates, and phosphates for special wastewater treatment applications.

Keywords: allophane; adsorption; precipitation; interface processes; environment; heavy metals; nano-structure; short-range order aluminosilicate; wastewater treatment; aqueous geochemistry

1. Introduction

Pollution of groundwater and drinking water by heavy metals is increasingly becoming a major environmental issue worldwide. Heavy metals are typically released by the weathering of rocks and minerals and from a wide range of human activities such as agriculture, energy production, manufacturing, transportation, mining, and waste disposal [1]. They often cause deleterious effects on aquatic life and to the terrestrial environment [2,3]. Contamination of surface water and groundwater with toxic and/or cancerogenic heavy metals and its subsequent use as a source of drinking water

without previous treatment is a major threat to human health [4–6]. To date, ~40% of the world's population suffers from water scarcity and lack access to unpolluted water or basic sanitation [7]. Consequently, there is a high demand for the development of new techniques and materials for wastewater treatment. In recent times, different techniques for the removal of aqueous metal ions have been developed and are routinely used in practice such as adsorption, precipitation, ion exchange, flocculation, sedimentation, membrane filtration, and electrochemical methods [8,9]. Contemporarily, natural, and synthetic macro-, micro-, and nano-adsorbents and nano-composites have been manufactured and are now successfully applied in water processing plants.

Generally, a small particle size (<10–100 nm), a large specific surface area (>10 m²/g), and the presence of surface functional groups (i.e., ≡Al–OH[°] and ≡Si–OH[°]) in adsorbents are favorable to ensure a desired adsorption rate and appropriate metal ion removal efficiency [10,11]. Recently, agricultural and industrial waste products, activated carbon nanotubes, cellulose, carbonates, Fe- and Al-oxyhydroxides, zeolites, phosphates, and clay minerals are used in the remediation of water that is severely polluted with persistent and hazardous components such as heavy metal ions, dyes, antibiotics, biocide compounds, and other organic chemicals [12–16]. The use of clay minerals for wastewater treatment can be advantageous over other sorbents because of their worldwide occurrence, low mining and processing costs, and outstanding physicochemical and surface properties, making clay materials suitable for selective ion exchange, adsorption, and catalyst uses [1,17,18].

The short range order aluminosilicate allophane (1–2SiO₂·Al₂O₃·5–6H₂O) is a naturally occurring clay mineral, which is distributed in volcanic ash layers and in soils worldwide. Allophane has a 3.5 to 5.0 nm sized hollow spherical structure with 0.3–0.5 nm sized defect sites (so-called perforations or pore regions) on its surface [19–21]. Allophane “nanoballs” are characterized by a high surface area (>300 m²/g). They are known to adsorb appreciable amounts of ionic or polar pollutants because of an amphoteric ligand capacity [17,22,23]. To date, the sorption properties of allophane have not been utilized in the remediation of wastewater. Basic studies are needed to explore the use of natural and synthetic allophanes for water clean-up, as literature dealing with the qualitative and quantitative assessment of the metal ion removal efficiencies and/or the determination of adsorption capacities of critical metal ions by allophanes is scarce. Specifically, only a few studies report on the preferential metal ion uptake by modified allophane (i.e., phosphate grafted), as discussed later in the paper, but there is an apparent knowledge gap with respect to the adsorption of potentially hazardous cations (e.g., Co, Ni, Zn, Pb) by chemically untreated allophanes. Moreover, although the prominent physical and electrochemical features of allophanes have been valued in earlier studies [10,11,17,18,21–23], it remains questionable as to whether metal ion removal from solution by allophanes follows chemical ion exchange or a physical adsorption process, or a combination of the two mechanisms. Hence, in this study, we investigated the adsorption kinetics and the mechanisms of the uptake of aqueous Ba, Co, Sr, and Zn species by Ecuadorian allophane and two synthetic allophanes at 25 °C as a function of contact time, pH, and metal ion concentration. It is shown that all types of allophane tested revealed a high affinity to adsorb metal cations over a wide pH range and exhibit sufficiently high adsorption capacities, as seen by a comparative study of critical adsorption parameters (e.g., pH, concentration ranges, contact time, surface properties of adsorbents) and economic considerations (e.g., estimated production costs for different allophanes) between untreated natural and synthetic allophanes and other currently available mineral adsorbents. Besides, the metal ion-specific adsorption rates and the removal efficiencies of allophanes are presented as a function of chemical key parameters and are discussed in relation to the potential use of allophane in special water processing technologies.

2. Materials, Experimental, and Methods

2.1. Materials

Allophane-rich soil material from the “allophane facies” of the Santo Domingo de los Colorados deposit in Ecuador (“NatAllo”) and two synthetic allophanes (“SynAllo-1” and “SynAllo-2”) were used

for the adsorption studies. NatAllo was used as received without further purification (sample 4–7; [24]). SynAllo-1 and SynAllo-2 were precipitated by modifying the method of Wada et al. [25]. Briefly, 1.0 L of a stock solution containing 100 mM of $\text{Si}(\text{OH})_4$ ($\text{Na}_2\text{SiO}_3 \cdot 2\text{H}_2\text{O}$ from Roth) was mixed with anhydrous AlCl_3 (SynAllo-1) or $\text{Al}(\text{NO}_3)_3 \cdot 9\text{H}_2\text{O}$ salts (SynAllo-2) from Roth to obtain an initial aqueous molar Al/Si ratio of 1. The two different Al salts have been used to evaluate the performance of synthetic allophanes made of “costly versus cost-reduced” raw materials (i.e., the commercial price for $\text{Al}(\text{NO}_3)_3 \cdot 9\text{H}_2\text{O}$ is about 20% less than for AlCl_3 per 1000 g). The experimental solution was adjusted to $\text{pH } 6.0 \pm 0.1$ using a 0.1 M NaOH solution and mingled at 150 rpm for 2 h using a magnetic stirrer at 25 °C. Subsequently, the experimental solution was aged at 80 °C in a compartment drier within the sealed high-density polyethylene batch reactor. After 48 h, the experiments were terminated. The solids were separated by a 0.45 μm filter (Sartorius, cellulose acetate) using a suction filtration unit, washed with deionized water to remove electrolytes, and dried at 40 °C.

For the adsorption experiments, individual stock solutions of Ba(II), Co(II), Sr(II), and Zn(II) were prepared by the dissolution of analytical grade chemicals ($\text{BaCl}_2 \cdot 2\text{H}_2\text{O}$, $\text{CoCl}_2 \cdot 6\text{H}_2\text{O}$, and NaCl from Roth; $\text{SrCl}_2 \cdot 6\text{H}_2\text{O}$ and ZnCl_2 from Merck) in deionized water (Milli-Q Plus UV, Millipore, Burlington, MA, USA, 18.2 M Ω at 25 °C). Each stock solution contained 230 mg/L (10 mM) of NaCl as background electrolyte.

2.2. Adsorption Experiments

Batch experiments were carried out to evaluate the effect of contact time, pH, and initial metal ion concentration on the adsorption capacity and on the rate of aqueous Ba, Co, Sr, and Zn removal by natural and synthetic allophanes at 25 °C. The effect of contact time on the adsorption behavior of aqueous metal ions by allophane was studied in a first set of experiments conducted at a constant pH of either 8.5 or 5.5, each ± 0.1 pH units. These experiments were carried out in 1.5 L high-density polyethylene reactors containing 1000 mL of the adsorbate (10 mg/L) and 2.0 g of the adsorbent. Immediately after placing the allophane in the reactor, the experimental solutions were adjusted to pH 8.5 or 5.5 with 0.1 M NaOH or 0.05 M HCl solutions. Fluid sampling (~1 mL) started instantly after the adjustment of the target pH value. Samples were taken after 10 s, 30 s, 1 min, 3 min, 5 min, 10 min, 1 h, and 1 day using a syringe (B. Braun, Omnifix® Solo, Melsungen, Germany), filtered via 0.45 μm cellulose acetate filters (Sartorius, Göttingen, Germany) and acidified using HNO_3 of suprapure grade (Roth, ROTIPURAN®, Karlsruhe, Germany).

The effect of pH on the uptake of aqueous metal ions by natural and synthetic allophanes was studied in a second set of batch experiments in the pH range from 8.5 to 4.0. The pH of the allophane suspensions was allowed to drift to a constant value (pH ~7–8), which required less than 1 h. The suspensions were then adjusted to $\text{pH } 8.5 \pm 0.1$ with 0.1 M NaOH solutions. All suspensions were stirred at 150 rpm for 2 h to ensure both the complete surface rehydration of the allophanes and the establishment of adsorption equilibrium between adsorbent and adsorbate. Afterwards, droplets of a 0.05 M HCl solution were added to the experimental solution to induce a pH decrease from 8.5 ± 0.1 to 4.0 ± 0.2 . The stepwise addition of the acid and fluid sampling (~1 mL á ~0.5 pH units) caused less than ~1.3% change of the initial fluid volume in all experiments, and thus no corrections for the metal ion concentration in solution were made. All experiments were of short duration (<2 h) in order to minimize changes in the surface area and surface properties of the allophanes.

In a third set of experiments, the effect of metal ion concentration on the adsorption behavior of allophanes was investigated at $\text{pH } 8.5 \pm 0.1$ for 2 h using 0.1 g of the adsorbent and 50 mL of solution containing Ba, Co, Sr, and Zn in different concentrations (1, 10, 20, 50, and 100 mg/L). The suspensions were prepared in analogy to those from the second set of experiments. The fluid sampling strategy was identical to the procedure described above.

The amount of metal ions adsorbed on the allophanes (q_e : mg/g) was calculated using Equation (1):

$$q_e = \frac{(C_0 - C_e)}{m} \times V \quad (1)$$

where c_0 and c_e are the initial and the equilibrium concentrations of the adsorbate (mg/L), m is the dry mass of the adsorbent (g), and V is the volume of the adsorbate solution (L).

The adsorption efficiency (% removal) is expressed by the percentage of removed adsorbate at equilibrium, according to Equation (2):

$$\%removal = \frac{(C_0 - C_e)}{C_0} \times 100 \quad (2)$$

2.3. Analytical Methods

2.3.1. Fluid-Phase Characterization

The solution pH was measured at 25 °C with a SenTix 41 glass electrode connected to a WTW Multi 350i pH-meter, which was calibrated against NIST buffer standard solutions at pH 4.01, 7.00, and 10.00 (analytical error: ± 0.05 pH units).

The total concentrations of aqueous Al, Ba, Co, Na, Si, Sr, and Zn were analyzed in acidified samples by inductively coupled plasma optical emission spectroscopy (ICP-OES) using a PerkinElmer Optima 8300 (Waltham, MA, USA). The analytical precision (2σ , 3 replicates) of the ICP-OES measurements was determined as $\pm 2\%$ for Ba, Na, Si, and Sr analyses and $\pm 3\%$ for Al, Co, and Zn analyses, respectively, relative to the NIST 1640a and SPS-SW2 Batch 130 standards.

The aqueous speciation of the solutions and the saturation degrees of the metal oxyhydroxides of Ba(II), Co(II), Sr(II), and Zn(II) were calculated using the PHREEQC software for Windows (version 2.18.00) in combination with its implemented Lawrence Livermore National Laboratory (LLNL) database at the experimental pH and temperature.

2.3.2. Solid-Phase Characterization

The mineralogy of the adsorbent materials was examined by X-ray diffraction (XRD) using a PANalytical X'Pert PRO diffractometer (Almelo, the Netherlands, Co-K α radiation) operated at 40 kV and 40 mA and outfitted with a spinner stage, 0.5° antiscattering slit, 1° divergence slit, primary and secondary soller, and a high-speed Scientific X'Celerator detector. The specimens were examined in the range 4–85° 2 θ with a step size of 0.008° 2 θ and a counting time of 40 s per step. Mineral quantification was carried out by Rietveld refinement of the XRD patterns using the PANalytical X'Pert Highscore Plus software package (version 2.2e, Almelo, the Netherlands) and a pdf-4 database.

Attenuated total reflectance Fourier transform infrared (ATR-FTIR) spectroscopy data were obtained for further characterization of the allophanes by a PerkinElmer Frontier FTIR (Waltham, MA, USA). Mid-infrared (MIR) spectra were recorded in the range from 4000–650 cm⁻¹ at a resolution of 2 cm⁻¹.

The specific surface area of the natural and synthetic allophanes before and after the adsorption experiments was analyzed on dried (100 °C for 24 h) aliquots by the multi-point adsorption BET method using a Micrometrics FlowSorb II2300 (Norcross, GA, USA) and a He(69.8)–N₂(30.2) mixture as the carrier gas. The estimated analytical uncertainty is $\pm 10\%$.

The particle shape, the nano-structure, and the geochemical composition of the allophanes were analyzed by transmission electron microscopy (TEM) on a FEI Tecnai F20 (FEI, Hillsboro, OR, USA) operated at an accelerating voltage of 200 kV. This instrument is fitted with a single-crystal LaB₆ Schottky Field Emitter, a Gatan imaging filter, an UltraScan CCD camera for high-resolution imaging and selected area electron diffraction (SAED), and an EDAX Sapphire Si(Li) detector for energy-dispersive X-ray spectroscopy (EDX) analysis. The TEM-EDX spectra were acquired using a counting time of 30 s to reduce element migration and element loss. The accuracy of the EDX results was verified by replicate measurements performed on a suite of phyllosilicate standards [26–28]. The analytical error was determined to be ± 2 at.% for Si and Al analyses.

3. Results and Discussion

3.1. Mineralogical Characterization of Allophane Adsorbents

XRD analysis confirmed the dominance of allophane in NatAllo (~78 wt.%; [24,29]), which also contains minor quantities (each <5 wt.%) of quartz, cristobalite, feldspar (albite and orthoclase), hornblende, halloysite, gibbsite, and goethite (Figure 1). The XRD patterns of SynAllo-1 and SynAllo-2 exhibited two broad peaks centered at ~3.4 Å and ~2.3 Å, which is typical for short-range ordered aluminosilicates such as allophane. No indication for the formation of amorphous silica or discrete Al–O–OH phases such as boehmite and gibbsite was found in the synthetic precipitates, implying that SynAllo-1 and SynAllo-2 consist solely of allophane. However, in these samples, the presence of traces of amorphous Al-hydroxides cannot be excluded. The XRD patterns of natural and synthetic allophanes sorbed with Zn²⁺ ions (for the experiments with aqueous Ba, Co, and Sr, similar patterns were obtained, but are not shown) do not reveal the formation of discrete Ba(II), Co(II), Sr(II), and Zn(II) oxyhydroxides, suggesting that chemical precipitation is negligible.

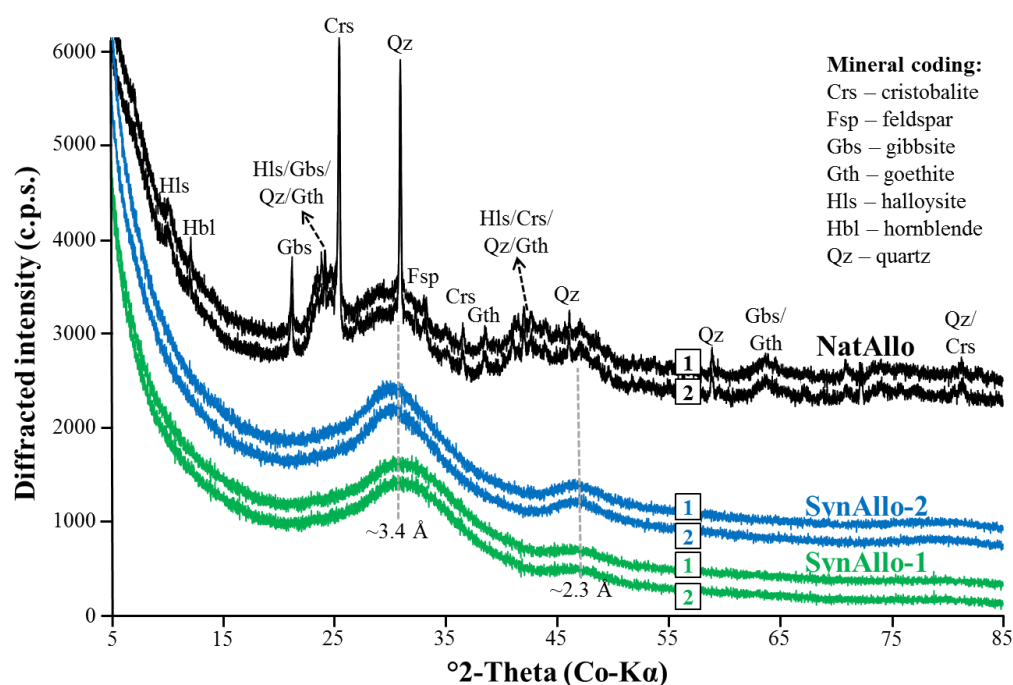


Figure 1. X-ray diffraction (XRD) patterns of Ecuadorian allophane (NatAllo) and synthetic allophanes (SynAllo-1 and SynAllo-2) used as adsorbents before the adsorption experiments (1) and with sorbed Zn²⁺ ions (2). Peaks at ~3.4 Å and ~2.3 Å correspond to allophane.

The MIR spectra of the allophanes before and after the adsorption experiments displayed very similar profiles. Figure 2 presents IR spectra of unreacted allophane and with sorbed Zn²⁺ ions (for experiments with aqueous Ba, Co, and Sr, similar spectra were obtained, but are not shown). The IR bands of the metal ions adsorbed could not be resolved, because the adsorbate concentration is low relative to that of the adsorbent. The presence of halloysite in NatAllo is indicated by two IR bands in the OH-stretching region (3600–3700 cm⁻¹). In addition, gibbsite and quartz were identified in this sample, which matches with the XRD results. The main lattice vibration bands of the allophanes are located between 1000–980 cm⁻¹ and at 870 cm⁻¹ due to Si–O–(Si) or Si–O–(Al) vibrations and Si–OH groups [19,30,31]. The IR spectra of SynAllo-1 and SynAllo-2 are similar to those reported for natural allophane, which shows that proto-imogolite allophane or imogolite structures did not form under the given experimental conditions [19,25,32].

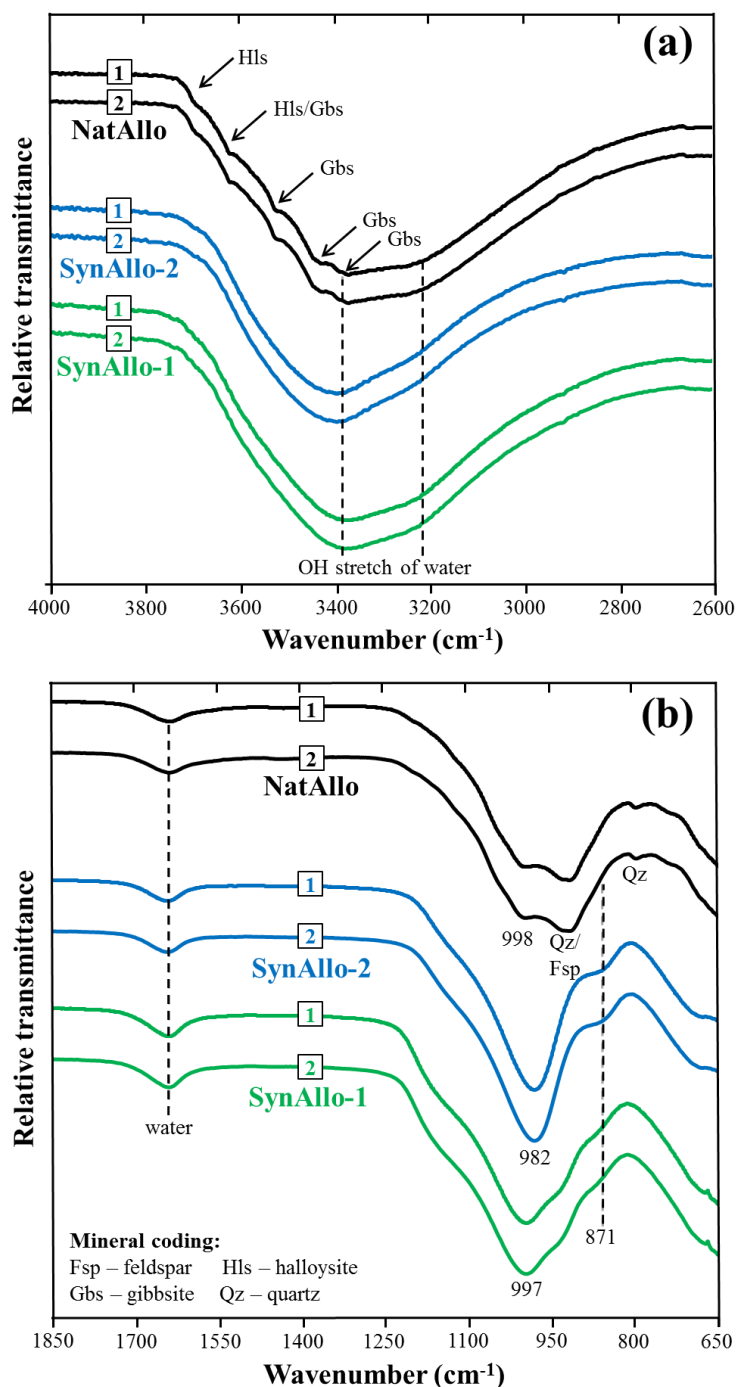


Figure 2. Attenuated total reflectance Fourier transform infrared (ATR-FTIR) spectra of NatAllo, SynAllo-1, and SynAllo-2 before the adsorption experiments (1) and with sorbed Zn²⁺ ions (2). (a) Hydroxyl stretching region; (b) lattice vibration region.

3.2. Structural and Chemical Characterization of Allophane Adsorbents

Representative TEM images of allophane nano-particles are shown in Figure 3. The allophane particles from NatAllo, SynAllo-1, and SynAllo-2 are 5 ± 2 nm, 8 ± 3 nm, and 10 ± 5 nm, on average, in largest dimension and have an aspect ratio equal to 1. The SAED patterns of natural and synthetic allophanes display weak diffraction rings or smeared Bragg patterns (Figure 3e,f), which is typical for short-range ordered aluminosilicates, that is, allophane. Such allophane structures are often described as ring-shaped, hollow spherules or allophane nano-balls [19,31].

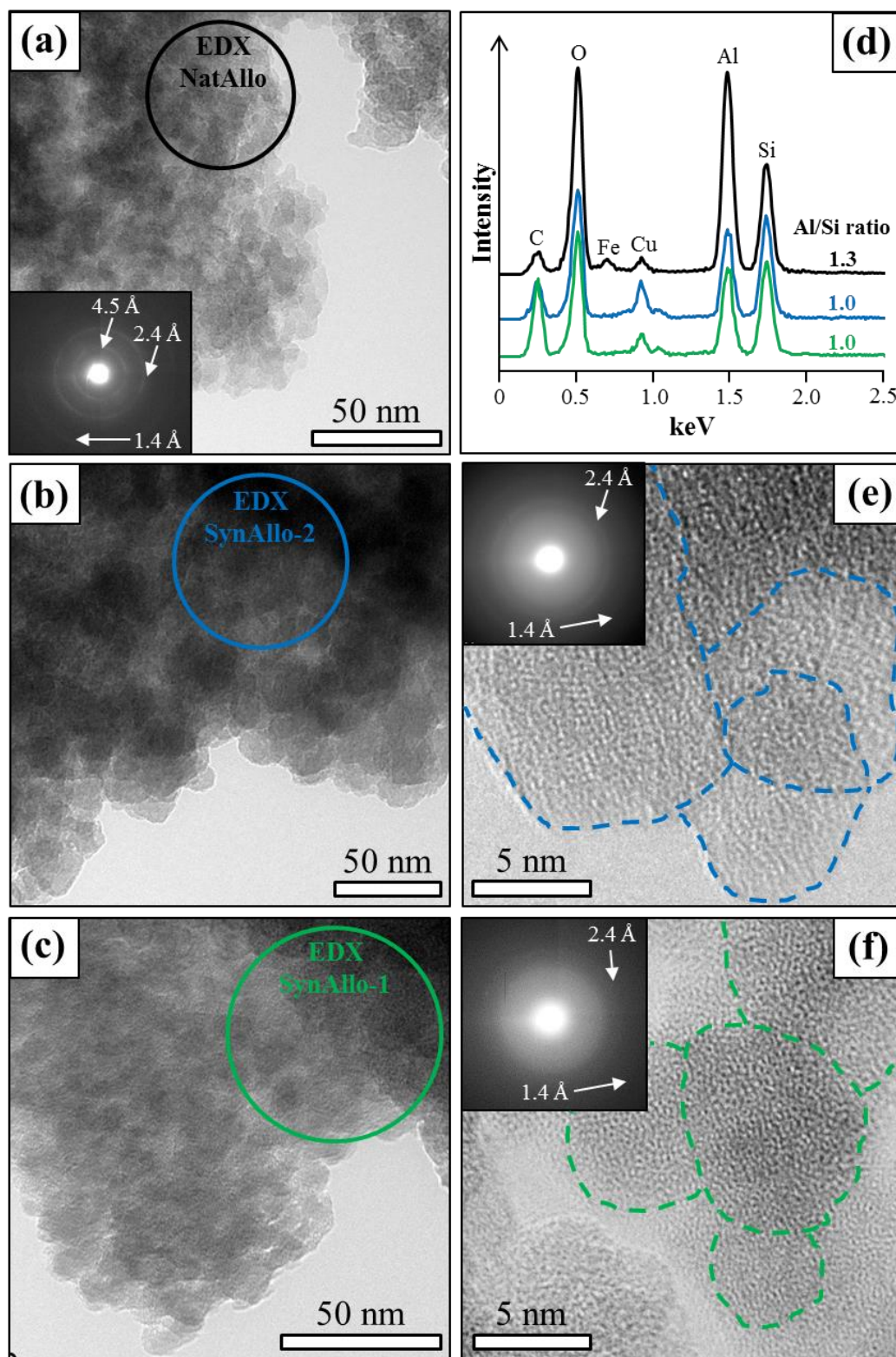


Figure 3. Transmission electron microscopy (TEM) images and selected area electron diffraction (SAED) patterns of allophane nano-particles used as adsorbents. (a) NatAllo; (b) SynAllo-2; (c) SynAllo-1. (d) TEM-energy-dispersive X-ray spectroscopy (EDX) spectra and corresponding averaged atomic Al/Si ratios of natural and synthetic allophanes (spot positions are marked in a–c). The small Fe peak indicates the presence of goethite in NatAllo. (e,f) High-resolution TEM lattice fringe images and related SAED patterns of SynAllo-2 and SynAllo-1, respectively, displaying allophane “nano-ball” structures.

The specific surface areas are 294 m²/g for NatAllo, 358 m²/g for SynAllo-1, and 370 m²/g for SynAllo-2, respectively. These values are in the range of N₂-BET values previously reported for natural allophanes (~200–400 m²/g) and synthetic allophanes (~250–900 m²/g) [10,29,33]. It is noteworthy that the BET values obtained before and after the adsorption experiments were identical to within the analytical precision of the BET analyses, which indicates that changes in the surface area and surface properties of the adsorbents are negligible throughout the experiments.

Allophanes are classified by their atomic Al/Si ratio, with Al-rich proto-imogolite allophane or imogolite-like allophanes (Al/Si = 2) and Si-rich halloysite-like or pumice allophanes (Al/Si = 1) as the members [19]. TEM-EDX analysis of cloud-like particle aggregates of NatAllo yielded an averaged atomic Al/Si ratio of 1.3 ± 0.2 (Figure 3d), corroborating the atomic Al/Si ratio of 1.3–1.4 for Ecuadorian allophane previously reported in Kaufhold et al. [24]. Such allophanes are very often referred to as “stream deposit allophanes” or “silica springs allophane”, according to Parfitt [19]. Minor amounts of Fe in NatAllo (Figure 3d) most likely belong to fine-grained goethite particles, being dispersed in the allophane aggregates. The atomic Al/Si ratio of the synthetic allophanes was determined as 1.0 ± 0.1 (Figure 3d), which is close to the Si-rich member.

3.3. Structural and Chemical Characterization of Allophane Adsorbents

3.3.1. Aqueous Speciation of Metal Ions Used as Adsorbates

The affinity between a chemical component and the adsorbent controls the extent at which an aqueous metal ion is adsorbed onto a mineral surface. Indeed, the aqueous speciation of a metal ion, pH, contact time, temperature, and the metal ion concentration are important factors that determine the kinetics and the efficiency of a given adsorption process [8,12,13,33]. In these experiments, the aqueous speciation of Ba and Sr was predominated by “free” Ba²⁺ and Sr²⁺ ions at pH 8.5 to 4.0. Minor quantities (<2%) belonged to BaCl⁺ and BaOH⁺ versus SrCl⁺ and SrOH⁺ aquo-complexes, which indicates that the vast majority of the total Ba and Sr species prevailed in the cationic form. In contrast, the aqueous speciation of Co and Zn was characterized by the sole presence of HCoO₂⁻ and by the dominance of Zn²⁺ (61%), Zn(OH)₂⁰ (19%), ZnOH⁺ (16%), ZnCl⁺ (3%), and Zn(OH)Cl (1%) aquo-complexes at pH 8.5. At pH ≤ 6.5 for Co and at pH ≤ 7.5 for Zn, however, the Co²⁺ and Zn²⁺ species dominated over trace amounts (<5%) of HCoO₂⁻, CoCl⁺, and Co(OH)₂⁰ versus ZnCl⁺, ZnOH⁺, Zn(OH)₂⁰, and Zn(OH)Cl aquo-complexes. From these data, it can be inferred that significant changes in the aqueous speciation of Co and Zn did occur in the pH-drift experiments.

All experimental solutions were undersaturated with respect to the least soluble oxyhydroxides of Ba(II), Co(II), and Sr(II) at any time throughout the experiments. However, in the case of aqueous Zn, the experimental solutions were oversaturated with respect to both the Zn(OH)₂ polymorphs and Zn₂(OH)₃Cl at pH ≥ 7.3, although none of the latter phases has been detected by XRD and FTIR analyses (Figure 2), which indicates that metal ion removal by chemical precipitation is insignificant.

3.3.2. Effect of Contact Time on the Adsorption Kinetics of Aqueous Metal Ions

The effect of contact time on the adsorption behavior of aqueous Ba, Co, Sr, and Zn by allophane adsorbents was investigated at pH values of either 8.5 or 5.5 (reflecting the observed minimum and maximum adsorption efficiencies; see Section 3.3.3.). It can be inferred from Figure 4 that the metal ion uptake by allophane increased significantly within 3–5 min, but it slowed down afterwards because of both a decrease in the binding sites of the adsorbents and a decrease in the metal ion concentration in solution. More specifically, for aqueous Ba, Sr, and Zn, adsorption has been completed within less than 5 min at pH 8.5 (Table 1), while aqueous Co needed 10 min to reach equilibrium. As expected, the removal efficiency strongly decreased and the time to reach adsorption equilibrium increased at decreasing pH (Table 1). This is because the ≡Al–OH^o and ≡Si–OH^o groups are more protonated under acidic conditions and potential binding sites are less available to retain metal ions [30].

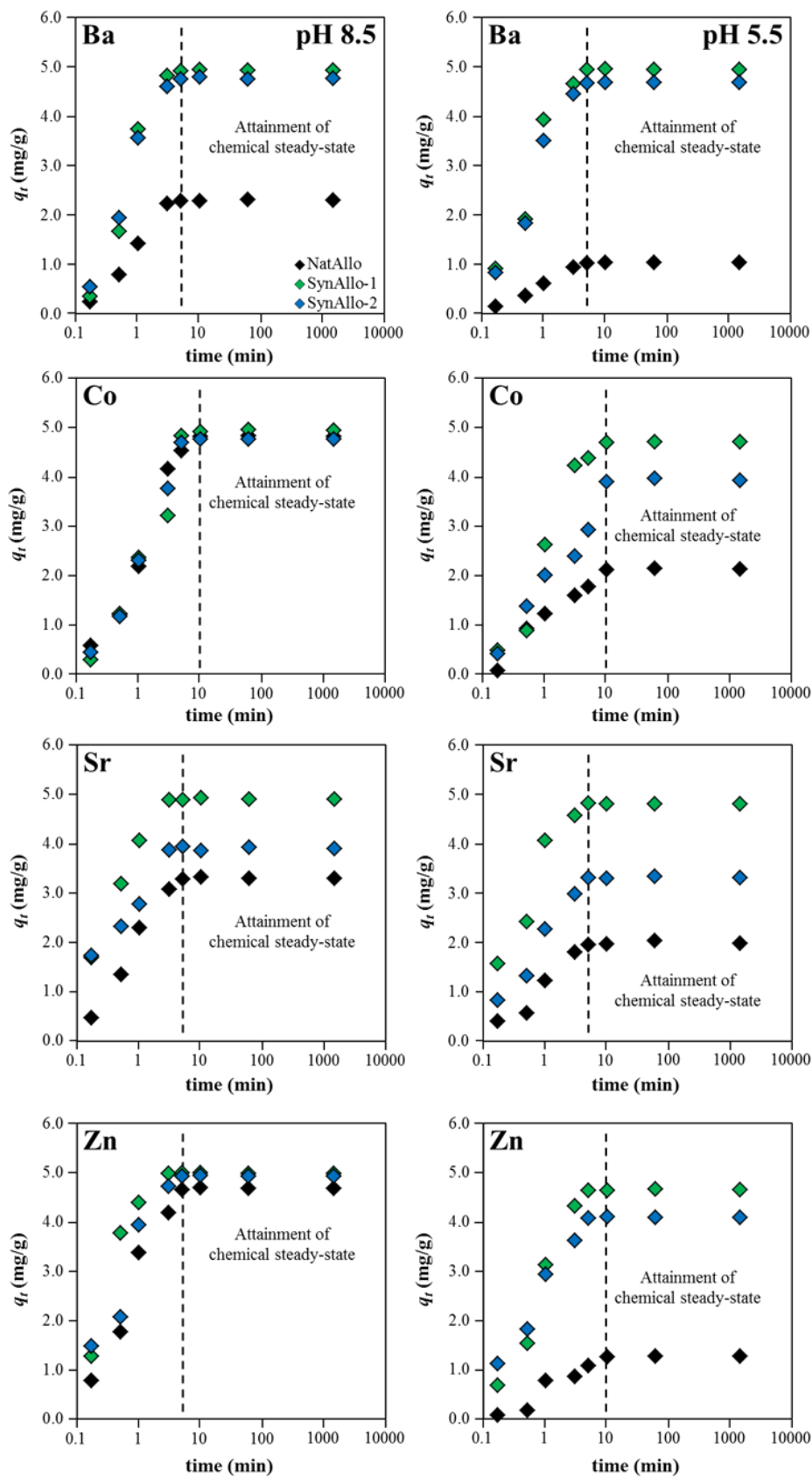


Figure 4. Effect of contact time on the adsorption behavior of aqueous metal ions (initial concentration: 10 mg/L; temperature: 25 °C) by natural and synthetic allophanes at pH 8.5 (left panel) and pH 5.5 (right panel).

Table 1. Comparison of measured (q_e^\dagger) and calculated (q_e^\ddagger) adsorption capacities obtained from pseudo-first-order (PFO) kinetic model parameters, and compilation of equilibration time (Equil. time) and metal ion removal efficiencies for all allophane adsorbents at pH 8.5 (upper part) and pH 5.5 (lower part).

Adsorbent	Adsorbate at pH 8.5	Equil. Time (min)	q_e^\dagger (mg/g)	Removal Rate (% Removal)	Pseudo-First Order Parameters		
					K (1/min)	q_e^\ddagger (mg/g)	R ² (–)
NatAllo	Ba ²⁺	5	2.3	45.2	1.090	2.5	0.996
	[HCoO ₂] [−]	10	4.8	95.3	0.573	4.6	0.988
	Sr ²⁺	5	3.3	65.8	0.948	3.1	0.994
	Zn ²⁺	5	4.7	93.5	0.953	4.9	0.953
SynAllo-1	Ba ²⁺	5	4.9	97.1	1.179	4.9	0.992
	[HCoO ₂] [−]	10	4.9	97.6	0.580	4.9	0.942
	Sr ²⁺	3	4.9	97.9	2.003	5.0	0.996
	Zn ²⁺	3	5.0	99.8	2.291	4.9	0.996
SynAllo-2	Ba ²⁺	5	4.8	93.9	1.150	4.8	0.997
	[HCoO ₂] [−]	10	4.8	94.2	0.676	4.8	0.977
	Sr ²⁺	3	3.9	77.9	1.667	3.8	0.978
	Zn ²⁺	5	4.9	98.6	1.271	4.8	0.977
Adsorbent	Adsorbate at pH 5.5	Equil. Time (min)	q_e^\dagger (mg/g)	Removal Rate (% removal)	Pseudo-First-Order Parameters		
					K (1/min)	q_e^\ddagger (mg/g)	R ² (–)
NatAllo	Ba ²⁺	5	1.0	20.4	0.953	1.1	0.989
	Co ²⁺	10	2.1	42.3	0.475	2.0	0.957
	Sr ²⁺	5	2.0	39.8	0.875	2.0	0.994
	Zn ²⁺	10	1.3	25.4	0.462	1.3	0.965
SynAllo-1	Ba ²⁺	5	5.0	97.4	1.134	4.8	0.971
	Co ²⁺	10	4.7	93.3	0.635	4.6	0.984
	Sr ²⁺	5	4.8	96.4	1.348	4.6	0.942
	Zn ²⁺	5	4.7	93.0	0.986	4.9	0.990
SynAllo-2	Ba ²⁺	5	4.68	92.1	1.162	4.81	0.986
	Co ²⁺	10	3.93	78.0	0.437	4.12	0.925
	Sr ²⁺	5	3.32	66.4	1.046	3.51	0.952
	Zn ²⁺	5	4.09	81.7	1.014	3.98	0.940

The kinetics of the metal ion uptake by allophane was described by a pseudo-first-order (PFO) model [16,34], according to Equation (3):

$$\ln(q_e - q_t) = -k \cdot t + \ln(q_e) \quad (3)$$

where q_e and q_t are the amounts of adsorbate uptake per mass of adsorbent (mg/g) at equilibrium and at time t (min), and k (1/min) is the rate constant of the PFO function. It is noteworthy that the plot of Equation (3) is linear and the calculated and measured q_e values match perfectly (slope: 0.998; $n = 24$; $R^2 = 0.987$), which proves the ability of the PFO model to fit the experimental data [16]. The calculated values for k and q_e are reported in Table 1.

It can be seen from the kinetic data that metal ion uptake is an exceptionally fast process, which suggests a high affinity of all allophanes to specifically adsorb metal ions. Furthermore, one can see that 5–10 min is enough to achieve adsorption equilibrium under the experimental conditions used in this study, which indicates that physical adsorption rather than ion exchange mainly contributes to the removal of metal ions by natural and synthetic allophane adsorbents. This finding is in line with previous experimental results, where allophane has been successfully used in the remediation of aqueous solutions that were contaminated with, for example, heavy metals cations [15,22,33,35], metal (oxy)anions [18,23,30], heterocyclic organic components [10], anionic surfactants, and organic acids [17,23]. Unfortunately, in most of these works, high reaction times (e.g., 24 h or longer) have been used and no kinetic data are provided [10,15,18,22,23,30,35], which greatly complicates the comparison

of the adsorption kinetics of, for example, allophanic soils and synthetic allophanes. However, adsorption data for the uptake of Pb^{2+} , sodium linear alkylbenzene sulfonate, and anthracene by soil allophanes and synthetic allophanes [17,33] generally indicate that adsorption remained constant after 1 h or less, suggesting the uptake of different pollutants by allophanes proceeds very fast.

3.3.3. Effect of pH on Metal Ion Removal Efficiency

Metal ion uptake by allophane depends mainly on pH as acidity affects the aqueous speciation of the metal ions and the (de)protonation degree of the functional $\equiv\text{Al}-\text{OH}^\ominus$ and $\equiv\text{Si}-\text{OH}^\ominus$ groups at the allophane surface [19,30,35]. Figure 5 presents the evolution of the amounts of aqueous Ba, Co, Sr, and Zn adsorbed on allophane from pH 4.0 to 8.5. The corresponding metal ion removal efficiencies at pH 8.5 and pH 4.0 are reported in Table 1. Metal ion uptake by NatAllo was low at $\text{pH} \leq 5.0$, followed by an adsorbate-dependent increase at pH 5.5 to 7.5 and attained a maximum at $\text{pH} \geq 8.0$ (Figure 5). SynAllo-1 revealed the highest removal efficiency (i.e., $\geq 95\%$ removal) for aqueous Ba at pH 4.0–8.5, Sr at pH 4.5–8.5, Zn at pH 5.5–8.5, and Co at pH 6.0–8.5. SynAllo-2 displayed lower removal efficiencies than SynAllo-1, but it exhibited a good performance at $\text{pH} \geq 7.0$. NatAllo showed the highest pH-dependency for the metal ion uptake (Figure 5).

The obtained results reflect the affinity of the aqueous metal ions to bind to charged allophane surfaces and the tendency to hydrolyze [22]. Si-rich allophane (like SynAllo-1 and SynAllo-2) has a permanent (structural) negative charge, while Al-rich allophane (NatAllo) has a higher amount of variable (pH-dependent) charges [36], which could explain the pH-dependent metal ion uptake of NatAllo, relative to SynAllo-1 and SynAllo-2 (Figure 5). However, the allophane surface exhibits a positive charge under acidic conditions and thus the metal ion uptake is limited because of repulsive electrostatic forces below the point of zero charge (PZC) value [30]. Thus, net adsorption increases significantly towards near-neutral to alkaline conditions, close to or above the PZC value, which is 7.8 to 9.4 for synthetic allophanes and 5.5 to 6.5 for natural allophanes, as reported in the literature [21,30,31]. With respect to metal ion uptake from solution, the latter indicates that natural allophanes should perform better under near-neutral to slightly alkaline conditions (e.g., pH 6–9) than synthetic allophanes for the electrochemical reasons discussed above. Although comparative studies on the pH-dependency of the adsorption of aqueous metal ions by allophanes are scarce, experimental data typically reveal a better performance of the synthetic versus natural allophanes, even at lower pH values [10], corroborating the results obtained in this study (Figure 5). The reasons for this behavior are not completely understood yet, but the following influencing factors, besides apparent differences in atomic Al/Si ratios, PZC values, and surface areas, may be relevant; presence or absence of colloidal organic matter and Fe-oxyhydroxides in allophanic soils versus synthetic allophanes. In this line, the presence of trace amounts of goethite on the allophane surface could affect the surface (charge) properties of NatAllo (Figure 3), that is, blocking potential adsorption sites and thus lowering the efficiency of metal ion uptake. The small differences in the N_2 -BET values (294 to 370 m^2/g) cannot explain the large differences observed in the removal efficiencies of NatAllo, SynAllo-1 and SynAllo-2.

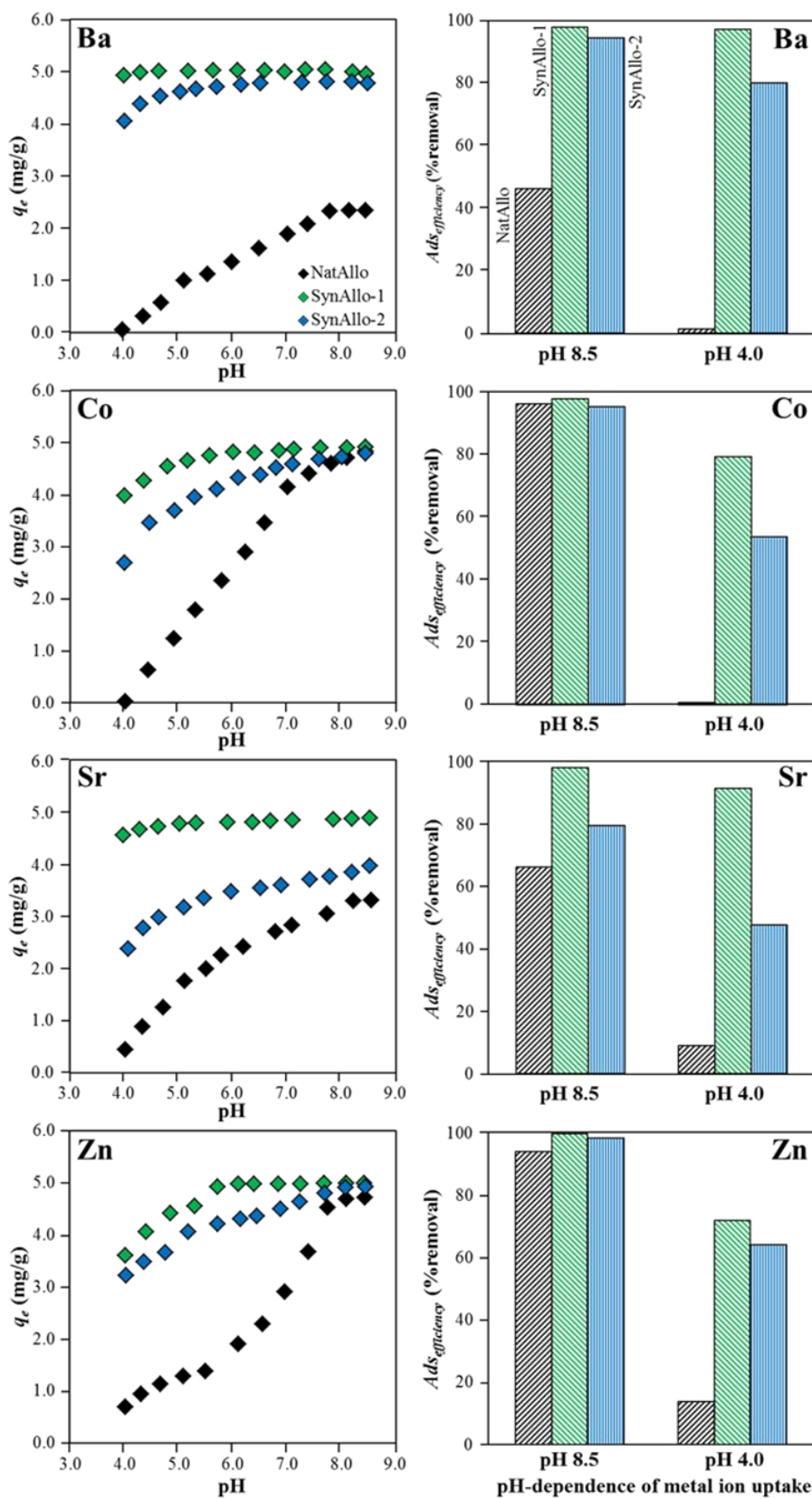


Figure 5. Adsorption of aqueous Ba, Co, Sr, and Zn by natural and synthetic allophanes as a function of pH (left panel). Effect of pH on the adsorption behavior of aqueous metal ions (right panel). Adsorption efficiencies at pH 8.5 versus pH 4.0.

3.3.4. Effect of Metal Ion Concentration on the Adsorption Efficiency

The metal ion concentration plays an important role on controlling the adsorption behavior of allophane. Figure 6 (left panel) shows that the adsorption efficiency increased almost proportionally at higher initial metal ion concentrations, but it slowed down at concentrations higher than 50 mg/L because of the progressive saturation of the binding sites on the allophane surfaces [13]. All allophanes exhibited highly metal ion-specific removal efficiencies. SynAllo-1 revealed a better adsorption for Ba^{2+} , Zn^{2+} , and Sr^{2+} than HCO_2^- ions, while SynAllo-2 showed a preferable uptake of Zn^{2+} over Ba^{2+} , HCO_2^- , and Sr^{2+} ions, and NatAllo displayed a better adsorption for Zn^{2+} relative to HCO_2^- , Ba^{2+} , and Sr^{2+} ions. The obtained results likely depend on the individual surface charge properties of the adsorbents (although not confirmed by our data), and in particular, on the aqueous speciation of the adsorbate [16,33,35,37]. The general observation that the uptake of aqueous metal ions by allophanes is component-specific, is in line with previous findings of Okada et al. [35], who showed that the adsorption by phosphate-grafted allophanes increased in the order $\text{Ni}^{2+} \leq \text{Mg}^{2+} < \text{Co}^{2+} < \text{Ca}^{2+} < \text{Zn}^{2+} < \text{Cu}^{2+}$ at pH 5.1–6.2. It has to be noted, however, that the selectivity of pollutant uptake by allophanes depends mainly on the individual experimental conditions used, that is, pH, temperature, aqueous concentrations, and speciation of the metal ions of interest and reaction time, as discussed before. Therefore, a comparison between adsorption efficiencies reported for certain metal ions and different allophane types and our data is problematic and should be made only with great caution.

3.3.5. Adsorption Isotherms and Adsorption Mechanism

Figure 6 (right panel) shows the plots of adsorption quantities versus the metal ion concentrations at equilibrium for the removal of aqueous Ba, Co, Sr, and Zn by the allophane adsorbents at pH 8.5. The isotherms initially increase sharply at low metal ion concentrations, which suggest that plenty of binding sites are available for adsorption. At higher metal ion concentrations, however, the curves become more flattened, which indicates that no more binding sites at the allophane surfaces are available for further adsorption and that a certain adsorption maximum has been reached. Over the last decades, a huge variety of models have been developed to describe adsorption isotherms, but the most commonly used models are the Langmuir, Freundlich, Dubinin–Radushkevich (D–R), and Redlich–Peterson models. The advantages, disadvantages, and limitations of these models are discussed in detail in the review paper by Tran et al. [16]. In this study, the Langmuir equation and the D–R model are used to describe the isotherms, because these models are considered to properly describe the adsorption on porous and heterogeneous materials with known surface characteristics, as for allophane. The linear form of the Langmuir model [38] is defined as Equation (4).

$$\frac{C_e}{q_e} = \frac{1}{K_L \cdot Q_{max}^0} + \frac{C_e}{Q_{max}^0} \quad (4)$$

where Q_{max}^0 denotes the maximum monolayer adsorption capacity of an adsorbent (mg/g) and K_L is the Langmuir adsorption constant (L/mg), which is related to the affinity between the adsorbent and the adsorbate. The values for Q_{max}^0 and K_L were computed from the slope and the interception of the linearized plots of C_e/q_e versus C_e and are reported in Table 2. From these values, one can see that the obtained adsorption data are adequately described by the Langmuir model. Following the recommendations of Tran et al. [16], the separation factor R_L (which is sometimes referred to as the equilibrium parameter) has been calculated, according to Equation (5).

$$R_L = \frac{1}{1 + K_L \cdot C_0} \quad (5)$$

The separation factor is a dimensionless constant, which describes the shape of an isotherm in a given solid–liquid adsorption system. An adsorption process is irreversible at $R_L = 0$, favorable at 0

$< R_L < 1$, linear at $R_L = 1$, and unfavorable at $R_L > 1$. The R_L values are shown in Table 2 and indicate that metal ion adsorption by allophane was favorable for all metal ion concentrations.

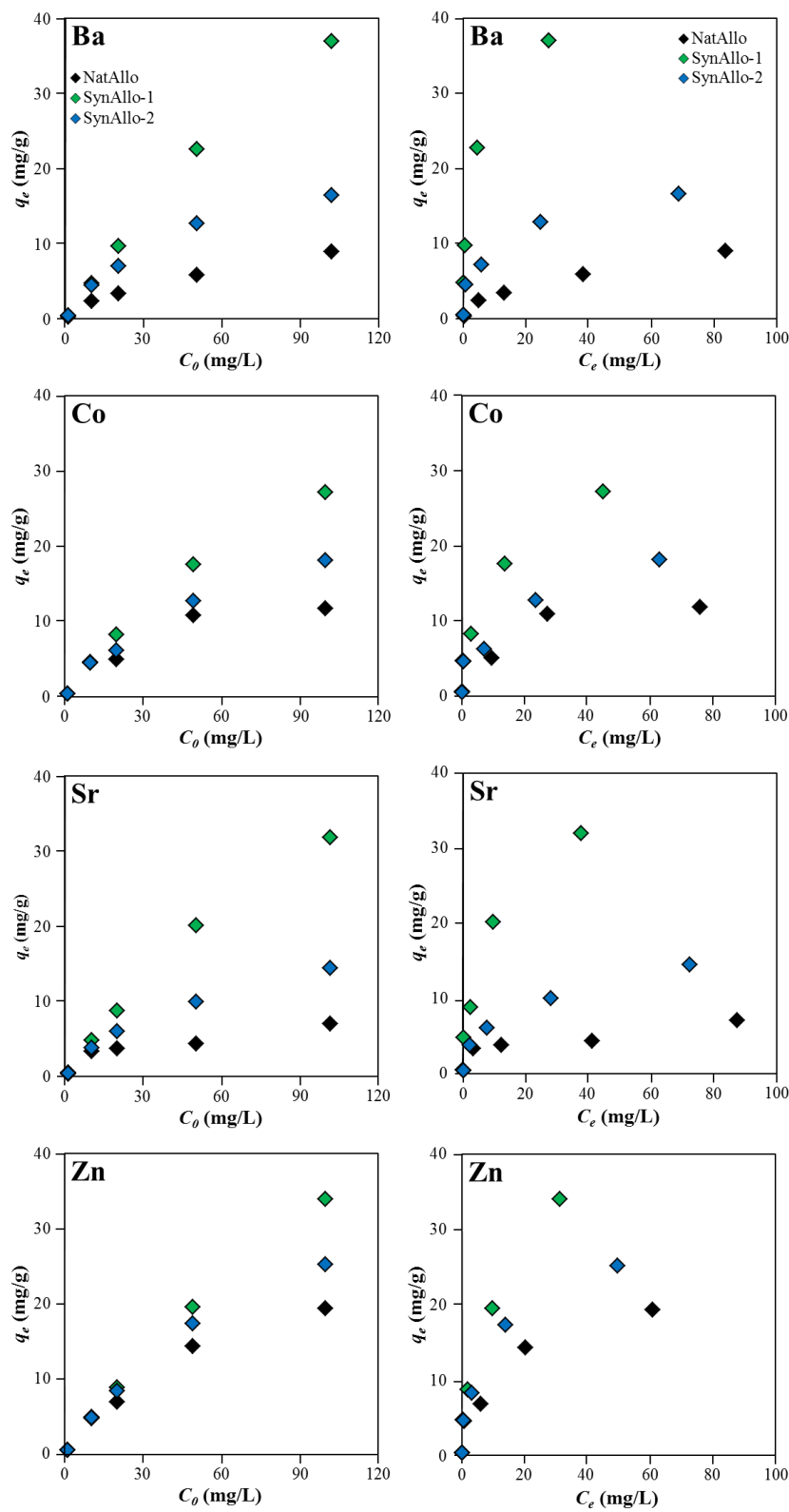


Figure 6. Adsorption behavior of aqueous Ba, Co, Sr, and Zn by natural and synthetic allophanes as a function of metal ion concentration. (left panel) Effect of initial metal ion concentration. (right panel) Adsorption isotherms at pH 8.5 and 25 °C.

Table 2. Langmuir isotherm parameters and separation factor (R_L) for the adsorption of aqueous Ba, Co, Sr, and Zn by natural and synthetic allophanes.

Adsorbent	Adsorbate at pH 8.5	Langmuir Parameters			R_L (–)
		Q^0_{max} (mg/g)	K_L (L/mg)	R^2 (–)	
NatAllo	Ba ²⁺	10.6	0.049	0.947	0.17–0.95
	[HCoO ₂] [–]	12.4	0.213	0.974	0.05–0.82
	Sr ²⁺	7.2	0.105	0.927	0.09–0.91
	Zn ²⁺	20.9	0.163	0.971	0.06–0.85
SynAllo-1	Ba ²⁺	38.6	0.676	0.994	0.01–0.60
	[HCoO ₂] [–]	29.0	0.226	0.968	0.04–0.81
	Sr ²⁺	34.4	0.265	0.970	0.02–0.58
	Zn ²⁺	36.9	0.240	0.985	0.04–0.80
SynAllo-2	Ba ²⁺	17.2	0.219	0.985	0.04–0.82
	[HCoO ₂] [–]	19.3	0.147	0.948	0.06–0.87
	Sr ²⁺	15.9	0.103	0.977	0.09–0.91
	Zn ²⁺	26.9	0.237	0.983	0.04–0.80

The D–R isotherm model has been often used to describe sorption phenomena at homogeneous and heterogeneous surfaces. The linear forms of the D–R equation [39] can be written as Equations (6) and (7):

$$\ln(q_e) = -K_{DR} \cdot \varepsilon^2 + \ln(q_{DR}) \quad (6)$$

$$\varepsilon = R \cdot T \cdot \ln\left(1 + \frac{1}{C_e}\right) \quad (7)$$

where q_{DR} is the maximum monolayer adsorption capacity (mg/g); K_{DR} denotes the D–R model constant (mol^2/kJ^2) related to the mean free energy of adsorption per mole of adsorbate as it migrates to the surface of a given adsorbent from an infinite distance in the aqueous solution; ε is the Polanyi potential (J^2/mol^2); and R and T are the universal gas constant ($8.314 \cdot 10^3 \text{ kJ}/(\text{mol} \cdot \text{K})$) and the absolute temperature (K), respectively. The values for q_{DR} and K_{DR} are reported in Table 3. From the activity coefficient K_{DR} the mean free energy of the adsorption process is derived from Equation (8):

$$E = \frac{1}{\sqrt{2 \cdot K_{DR}}} \quad (8)$$

where E is the free energy change (kJ/mol), which is required to transfer one mole of aqueous metal ions to the adsorbent's surface. Typical values for E range from 8 to 16 kJ/mol, if the adsorption follows ion exchange, and <8 kJ/mol if physical adsorption dominates. The calculated E values are reported in Table 3 and indicate that metal ion uptake by allophane follows physical adsorption rather than chemical ion exchange. It has to be noted that the formation of metal bidentate and monodentate ligands with deprotonated surface OH groups and subsequent strong electrostatic interaction with the charged allophane surfaces could have also contributed to the net uptake of aqueous metal ions. Although the dimension of this mechanism cannot be resolved from the present datasets, such surface processes could explain in parts the large differences observed in the adsorption of aqueous Ba, Co, Sr, and Zn by allophanes (Figure 6). Future work should concentrate on describing and quantifying the proportions of metal ion removal by chemisorption and physical adsorption by natural and synthetic allophanes using, for example, synchrotron-based X-ray absorption fine structure spectroscopy studies. Moreover, incongruent dissolution of allophane and the subsequent precipitation of secondary Al–(Ba, Co, Sr, Zn)-phases or hydrous (Ba, Co, Sr, Zn)-aluminosilicates cannot be ruled out under the experimental conditions used in this study, although the aqueous Si and Al concentrations remained always below 0.9 and 0.4 mg/L, respectively, which is equivalent to

a theoretical dissolution quota of <0.3% for allophane. For these reasons, in the following sections, we use the term “sorption” to describe the uptake of aqueous metal ions by allophane.

It can be concluded from the shape of the linearized Langmuir and D–R isotherm plots and their correlation coefficients (R^2 values), that our experimental data fit better to the Langmuir model than to the D–R model. Accordingly, the sorption capacity of SynAllo-1 is 38.6 mg/g for Ba^{2+} , 29.0 mg/g for $HCoO_2^-$, 34.4 mg/g for Sr^{2+} , and 36.9 mg/g for Zn^{2+} , which is two to three times higher than the load of these metal ions on SynAllo-2 and NatAllo. The reasons for this may include differences in the amount and distribution of permanent and variable charges, Al/Si ratios, BET, and PZC values and presence of traces of goethite in NatAllo versus SynAllo-1 and SynAllo-2, as discussed in Section 3.3.3.

Table 3. Dubinin–Radushkevich parameters and mean free energy change (E) for the adsorption of aqueous Ba, Co, Sr, and Zn on natural and synthetic allophanes.

Adsorbent	Adsorbate at pH 8.5	Dubinin–Radushkevich Parameters			E (kJ/mol)
		q_{DR} (mg/g)	K_{DR} (mol ² /kJ ²)	R^2 (–)	
NatAllo	Ba^{2+}	7.4	1.480×10^{-8}	0.979	5.8
	$[HCoO_2]^-$	10.5	9.115×10^{-9}	0.929	7.4
	Sr^{2+}	6.2	1.315×10^{-8}	0.962	6.2
	Zn^{2+}	16.3	1.143×10^{-8}	0.966	6.6
SynAllo-1	Ba^{2+}	44.5	7.914×10^{-9}	0.996	7.9
	$[HCoO_2]^-$	21.8	1.008×10^{-8}	0.971	7.0
	Sr^{2+}	26.5	8.593×10^{-9}	0.977	7.6
	Zn^{2+}	27.4	1.012×10^{-8}	0.979	7.0
SynAllo-2	Ba^{2+}	15.1	7.892×10^{-9}	0.988	8.0
	$[HCoO_2]^-$	14.2	1.009×10^{-8}	0.948	7.0
	Sr^{2+}	12.4	1.384×10^{-8}	0.990	6.0
	Zn^{2+}	21.2	1.026×10^{-8}	0.983	7.0

3.4. Comparative Analysis of Sorption Capacities of Allophane and Other Materials

The sorption capacities of some other recently available sorbents for aqueous Ba, Co, Sr, and Zn are given in Table 4. It is evident that the sorption capacities of NatAllo, SynAllo-1, and SynAllo-2 for Ba^{2+} , $HCoO_2^-/Co^{2+}$, Sr^{2+} , and Zn^{2+} ions are equal or higher than most carbonates, phosphates, clay minerals, and zeolites, but are lower than goethite, activated carbons components, and nanoscale-Se, though such an evaluation is difficult for the reasons given below and discussed in De Gisi et al. [40].

Table 4. Comparison of the adsorption potential of natural and synthetic allophanes with other commercially available adsorbents used for the removal of aqueous Ba, Co, Sr, and Zn. Cpt = clinoptilolite; AGH = almond green hull; Mnt = montmorillonite; Bent = bentonite; TS = this study.

Adsorbate	Adsorbent	Q^0_{max} (mg/g)	Surface Area Particle Size	Conc. Range of Pollutant	Contact Time	T (°C)	pH	Ref.
Ba ²⁺	Ca-Cpt	15.3	<75 μm	0.005–0.1 N	168 h	-	-	[37]
	Ca-Mnt	15.3	<75 μm	0.005–0.1 N	48 h	-	-	[37]
	Dolomite	4.0	20 μm	10–50 mg/L	6 h	20–50	2.5–8.5	[41]
	Exp. perlite	2.5	1.9 m ² /g	5–50 mg/dm ³	6 h	20–50	2.0–7.0	[42]
	NatAllo	10.6	294.0 m ² /g	1–100 mg/L	2 h	25	8.5	TS
	SynAllo-1	38.6	358.0 m ² /g	1–100 mg/L	2 h	25	8.5	TS
	Syn-Allo-2	17.2	370.0 m ² /g	1–100 mg/L	2 h	25	8.5	TS
Co ²⁺ /HCoO ₂ ⁻	Al-pillared bent.	38.6	227.0 m ² /g	10–400 mg/L	24 h	30–60	2.0–9.0	[43]
	Kaolinite	11.0	11.6 m ² /g	10–250 mg/L	4 h	30	5.8	[44]
	Bent./Cpt mix	2.7	300–1000 μm	5–50 mg/L	12 h	-	-	[45]
	Goethite	86.6	2–10 nm	5–500 mg/L	1 h	30	5.0	[46]
	Lemon peel	22.0	150–200 μm	0–1000 mg/L	10 h	25	6.0	[47]
	NatAllo	12.4	294.0 m ² /g	1–100 mg/L	2 h	25	8.5	TS
	SynAllo-1	29.0	358.0 m ² /g	1–100 mg/L	2 h	25	8.5	TS
Syn-Allo-2	19.3	370.0 m ² /g	1–100 mg/L	2 h	25	8.5	TS	
Sr ²⁺	Act. carbon	44.4	>1200 m ² /g	10–200 mg/L	7–8 h	20–60	2.0–8.0	[48]
	AGH	116.3	<88 μm	161–635 mg/L	<0.1 h	25	7.0	[49]
	Dolomite	1.2	20 μm	10–50 mg/L	6 h	20–50	2.5–8.5	[42]
	Exp. perlite	1.1	1.9 m ² /g	5–50 mg/dm ³	6 h	20–50	2.0–7.0	[43]
	Cpt/CoFe ₂ O ₄	20.6	200–250 μm	20–400 mg/L	19 h	25–65	2.0–10.0	[50]
	NatAllo	7.2	294.0 m ² /g	1–100 mg/L	2 h	25	8.5	TS
	SynAllo-1	34.4	358.0 m ² /g	1–100 mg/L	2 h	25	8.5	TS
Syn-Allo-2	15.9	370.0 m ² /g	1–100 mg/L	2 h	25	8.5	TS	
Zn ²⁺	Act. phosphate	12.3	22.5 m ² /g	10–500 mg/L	2 h	10–40	5.0	[51]
	Chitosan	290.0	4.9 m ² /g	0–1000 mg/L	24 h	25	5.0	[52]
	Cpt	16.8	63–100 μm	100–600 mg/dm ³	24 h	25–65	6.0	[53]
	Kaolinite	4.9	12.8 m ² /g	50–2000 mg/L	120 h	20	4.5	[54]
	Nano-Se	62.1	80–260 nm	6–215 mg/L	16 h	30	6.5	[55]
	NatAllo	20.9	294.0 m ² /g	1–100 mg/L	2 h	25	8.5	TS
	SynAllo-1	36.9	358.0 m ² /g	1–100 mg/L	2 h	25	8.5	TS
Syn-Allo-2	26.9	370.0 m ² /g	1–100 mg/L	2 h	25	8.5	TS	

From the recent review paper by De Gisi et al. [40], it becomes clear that a direct comparison of adsorption data obtained from different sorbents is rather difficult, because of inconsistencies in the literature data and apparent differences in the test conditions and matrices used; thus, the accurate assessment of the applicability of (low-cost) sorbents for wastewater treatment is often delicate and should be valued separately for individual cases. As the test conditions used in this study, as well as the characteristics of the allophanes, are tendentially comparable with the specifications of the other materials (Table 4), we suppose that a qualitative evaluation between the different sorbents may be valid. In this light, the metal-ion specific sorption capacities obtained for the natural and synthetic allophanes are well in the range of adsorption data previously reported for agricultural, household, and industrial waste sorbents, as well as sludge, soil, and ore materials used for the removal of heavy metals [40].

3.5. Application of Allophane in Water Processing Technologies

A great variety of treatment technologies is currently available for wastewater purification [8,9]. Most of these techniques, that is, ion exchange, membrane filtration, and electrochemical methods, have high operational and maintenance costs and the toxic waste produced has to be disposed separately, causing economic and environmental problems. In wastewater treatment plants, critical pollutants (e.g., heavy metal ions) are nowadays removed from solution by biological conditioning or chemical oxidation; adsorption processes are also applied to extract contaminants that may remain in solution after passing the initial processing steps. Specifically, metal ion removal by adsorption is considered to be a good alternative in wastewater purification, because this method is easy-to-handle, simple and

relatively cost-efficient, compared with the other technologies [40]. At present, the most commonly used sorbents are activated carbon components. However, their use in wastewater treatment plants is sometimes restricted, mainly because of the higher costs (~US\$20–1000 up to US\$22,000 per ton), partly limited regeneration capacity, and lavish disposal after service life, compared with other low-cost adsorbents [8,9,40]. In this line, different raw materials and novel (nano-)composites have been examined in recent years for their applicability to remove hazardous metal ions from wastewater and to generally replace activated carbons.

Because of the very high affinity to bind aqueous metal ions, natural allophanes are good candidate materials to be used for the processing of solutions that are severely contaminated with persistent heavy metals. The high sorption capacity of NatAllo for PO_4^{3-} (37.5 mg/g), AsO_4^{3-} (17.6 mg/g), and F^- (3–5 mg/g) ions has already been proven, rendering this material suitable as an anion absorber [18,36]. The results obtained herein further indicate that natural and synthetic allophanes hold a great potential to effectively remove aqueous Ba, Co, Sr, and Zn over a wide pH range (Figure 5, Table 4). However, exploitable allophane deposits of high quality are relatively rare and estimated mining costs for the Ecuadorian allophane are in the range of ~US\$200–600 per ton; thus similar to halloysite, but significantly higher than other economic clay mineral deposits, such as the Wyoming bentonite (~US\$30–100 per ton) and Georgia kaolinite (~US\$50–400 per ton). Although a market for synthetic allophanes is barely there, the estimated manufacturing costs should be in the range of low-price to high purify synthetic zeolites, which is ~US\$300 up to US\$20,000 per ton. Therefore, the application of synthetic allophanes as sorbents in wastewater treatment plants is probably not yet sustainable. However, the applicability of using alternating layers of natural and synthetic allophanes and other low-cost sorbents (e.g., montmorillonite, geopolymers, and calcium–silicate-hydrates) in filter systems for water clean-up may be considered for a better cost-effectiveness [56–58].

From the application site, it is important to ensure a good performance, a proper workability, and a high robustness against modifications in surface charge and electrochemical properties, which could reduce the effectiveness of an adsorbent. Irreversible changes in the allophane properties can be induced during, for example, drying, grinding, heat treatment, and phosphate grafting [18,35]. For example, Kaufhold et al. [18] observed a lower F^- sorption capacity for calcined, granulated, and dried (at 60 °C) Ecuadorian allophane, compared with naturally moist material. Indeed, drying and heating can cause a decrease of the reactive $\equiv\text{Al}-\text{OH}^\circ$ groups through the formation of $\equiv\text{Al}-\text{O}-\text{Al}\equiv$ bridges between the allophane primary particles. This process is well-known to affect the surface acidity and decreases the sorption capacity of allophane [59]. Thus, drying of the allophanes could have led to an alteration of their surface (charge) properties, which partly explains the differences observed in their sorption capacities (Table 4). Further experiments with allophane suspensions and materials produced by using different drying and grinding methods have to be done to elucidate the effect of sample treatment on the metal ion removal efficiency and adsorption properties of natural and synthetic allophanes.

The evaluation of the adsorption behavior revealed that all allophane adsorbents tested in this study exhibited a performance equal or better than the other available mineral adsorbents such as zeolites, montmorillonite, carbonates, and phosphates used for the removal of aqueous Ba, Co, Sr, and Zn (Table 4). The XRD, FTIR, and TEM data (Figures 1–3) indicate that SynAllo-1 and SynAllo-2 consisted of pure allophane, causing a higher sorption capacity, compared with NatAllo. The sorption capacity of SynAllo-2 was lower than expected, particularly in view of its high allophane content and its highest specific surface area. This indicates that the sorption capacity does not solely depend on the purity of an adsorbent and that the specific surface area plays only a minor role. This finding is consistent with previous results [18,22,35], where the sorption efficiency was directly related to the amount of $\equiv\text{Al}-\text{OH}^\circ$ groups in allophane. Herein, it was impossible to quantify the $\equiv\text{Al}-\text{OH}^\circ$ groups because of the presence of halloysite in NatAllo and varying amounts of polymeric SiO_x attached on the octahedral sheet of the synthetic allophanes. A combination of PZC measurements, X-ray absorption fine structure spectroscopy methods, and in situ Raman techniques should be applied to

specify the surface charge characteristics of allophanes. In essence, allophane could be applied for remediating wastewater that is contaminated with hazardous metal ions, yet its operating efficiency has to be proven. In order to demonstrate the analogous performance of the allophane adsorbents under identical conditions with real metal ion ridden wastewater, further tests regarding the colloidal stability of allophane suspensions and the possibility to regenerate metal ion-loaded allophane (i.e., desorption and regeneration studies) have to be performed.

4. Conclusions

Natural allophane (NatAllo) from Ecuador and synthetic allophanes (SynAllo-1 and SynAllo-2) can be effectively used for the removal of aqueous Ba, Co, Sr, and Zn over a wide pH range (e.g., $5.5 \leq \text{pH} \leq 8.5$). Kinetic experiments revealed that the metal ion uptake by allophane reached equilibrium within less than 10 min at $4.0 \leq \text{pH} \leq 8.5$, and can be adequately described by a pseudo-first-order reaction kinetics. The Langmuir model described the adsorption behavior at equilibrium better than the Dubinin–Radushkevich model. The sorption capacity of SynAllo-1 was determined as 38.6 mg/g for Ba^{2+} , 29.0 mg/g for HCO_3^- , 34.4 mg/g for Sr^{2+} , and 36.9 mg/g for Zn^{2+} ions at pH 8.5, which is two to three times higher than for SynAllo-2 and NatAllo. The mean free energy of the adsorption process was calculated to be between 6 and 8 kJ/mol, which indicates that metal ion uptake by allophane is governed by physical adsorption rather than by chemical ion exchange. All allophane adsorbents tested showed sorption capacities comparable to other recently available materials such as zeolites, clay minerals, carbonates, and phosphates, and could thus be used for wastewater treatment because of their high adsorption capacity, worldwide occurrence, and low cost.

Author Contributions: Conceptualization, Investigation, Visualization, Writing—Original Draft Preparation, and Project Administration, A.B.; Experimental, A.B. and A.C.G., Methodology, Data Acquisition, and Curation, A.B., A.C.G., C.B., B.P., I.L.-P., S.K., and M.D.; Formal Analysis and Validation, A.B., C.B., and S.K.; Resources, M.D.; Supervision, A.B. and M.D.; Funding Acquisition, A.B. and M.D.

Funding: This research was partly funded by the NAWI Graz Geocentre, Graz University of Technology [F-AF7-221-01].

Acknowledgments: The authors are grateful to M. Hierz and A. Wolf (Graz University of Technology), who assisted us with the synthesis and adsorption experiments. F. Mittermayr (Graz University of Technology) is greatly acknowledged for conducting the BET measurements. The comments of two anonymous reviewers are highly appreciated.

Conflicts of Interest: The authors declare no conflict of interest.

References

1. Burakov, A.E.; Galunin, E.V.; Burakova, I.V.; Kucherova, A.E.; Agarwal, S.; Tkachev, A.G.; Gupta, V.K. Adsorption of heavy metals on conventional and nanostructured materials for wastewater treatment purposes: A review. *Ecotoxicol. Environ. Saf.* **2018**, *148*, 702–712. [[CrossRef](#)] [[PubMed](#)]
2. Bhuiyan, M.A.H.; Islam, M.A.; Dampare, S.B.; Parvez, L.; Suzuki, S. Evaluation of hazardous metal pollution in irrigation and drinking water systems in the vicinity of a coal mine area of northwestern Bangladesh. *J. Hazard. Mater.* **2010**, *179*, 1065–1077. [[CrossRef](#)] [[PubMed](#)]
3. Malik, Q.A.; Khan, M.S. Effect on Human Health due to Drinking Water Contaminated with Heavy Metals. *J. Pollut. Eff. Cont.* **2016**, *5*, 1000179. [[CrossRef](#)]
4. Crévecoeur, S.; Debacker, V.; Joaquim-Justo, C.; Gobert, S.; Scippo, M.L.; Dejonghe, W.; Martin, P.; Thomé, J.P. Groundwater quality assessment of one former industrial site in Belgium using a TRIAD-like approach. *Environ. Pollut.* **2011**, *159*, 2461–2466. [[CrossRef](#)] [[PubMed](#)]
5. Bacquart, T.; Frisbie, S.; Mitchell, E.; Grigg, L.; Cole, C.; Small, C.; Sarkar, B. Multiple inorganic toxic substances contaminating the groundwater of Myingyan Township, Myanmar: arsenic, manganese, fluoride, iron, and uranium. *Sci. Total. Environ.* **2015**, *517*, 232–245. [[CrossRef](#)] [[PubMed](#)]
6. Chabukdhara, M.; Gupta, S.K.; Kotecha, Y.; Nema, A.K. Groundwater quality in Ghaziabad district, Uttar Pradesh, India: Multivariate and health risk assessment. *Chemosphere* **2017**, *179*, 167–178. [[CrossRef](#)] [[PubMed](#)]

7. Calzadilla, A.; Rehdanz, K.; Tol, R.S.J. Water scarcity and the impact of improved irrigation management: a computable general equilibrium analysis. *Agric. Econ.* **2011**, *42*, 305–323. [[CrossRef](#)]
8. Fu, F.; Wang, Q. Removal of heavy metal ions from wastewaters: A review. *J. Environ. Manag.* **2011**, *92*, 407–418. [[CrossRef](#)] [[PubMed](#)]
9. Carolin, C.F.; Kumar, P.S.; Saravanan, A.; Joshiba, G.J.; Naushad, M. Efficient techniques for the removal of toxic heavy metals from aquatic environment: A review. *J. Environ. Chem. Eng.* **2017**, *5*, 2782–2799. [[CrossRef](#)]
10. Iyoda, F.; Hayashi, S.; Arakawa, S.; John, B.; Okamoto, M.; Hayashi, H.; Yuan, G. Synthesis and adsorption characteristics of hollow spherical allophane nano-particles. *Appl. Clay Sci.* **2012**, *56*, 77–83. [[CrossRef](#)]
11. Yuan, G.; Wada, S.I. Allophane and imogolite nanoparticles in soil and their environmental applications. In *Nature's Nanostructures*; Barnard, A.S., Guo, H.B., Eds.; Pan Stanford Publishing Pte Ltd.: Singapore, 2012; pp. 485–508, ISBN 9789814316828.
12. Babel, S.; Kurniawan, T.A. Low-cost adsorbents for heavy metals uptake from contaminated water: A review. *J. Hazard. Mater.* **2003**, *B97*, 219–243. [[CrossRef](#)]
13. Singha, A.S.; Guleria, A. Chemical modification of cellulosic biopolymer and its use in removal of heavy metal ions from wastewater. *Int. J. Biol. Macromol.* **2014**, *67*, 409–417. [[CrossRef](#)] [[PubMed](#)]
14. Ismadji, S.; Soetaredjo, F.E.; Ayucitra, A. Natural Clay Minerals as Environmental Cleaning Agents. In *Clay Materials for Environmental Remediation*; Ismadji, S., Soetaredjo, F.E., Ayucitra, A., Eds.; Springer Nature: Berlin, Germany, 2015; pp. 5–37, ISBN 978-3-319-16711-4.
15. Mukai, H.; Hirose, A.; Motai, S.; Kikuchi, R.; Tanoi, K.; Nakanishi, T.M.; Yaita, T.; Kogure, T. Cesium adsorption/desorption behavior of clay minerals considering actual contamination conditions in Fukushima. *Sci. Rep.* **2016**, *6*, 21543. [[CrossRef](#)] [[PubMed](#)]
16. Tran, H.N.; You, S.-J.; Hosseini-Bandegharai, A.; Chao, H.-P. Mistakes and inconsistencies regarding adsorption of contaminants from aqueous solutions: A critical review. *Water. Res.* **2017**, *120*, 88–116. [[CrossRef](#)] [[PubMed](#)]
17. Nishikiori, H.; Kobayashi, K.; Kubota, S.; Tanaka, N.; Fujii, T. Removal of detergents and fats from waste water using allophane. *Appl. Clay Sci.* **2010**, *47*, 325–329. [[CrossRef](#)]
18. Kaufhold, S.; Dohrmann, R.; Abidin, Z.; Henmi, T.; Matsue, N.; Eichinger, L.; Kaufhold, A.; Jahn, R. Allophane compared with other sorbent minerals for the removal of fluoride from water with particular focus on a mineable Ecuadorian allophane. *Appl. Clay Sci.* **2015**, *5*, 25–33. [[CrossRef](#)]
19. Parfitt, R.L. Allophane in New Zealand—A review. *Aust. J. Soil Res.* **1990**, *28*, 343–360. [[CrossRef](#)]
20. Hashizume, H. Adsorption of nucleic acid bases, ribose, and phosphate by some clay minerals. *Life* **2015**, *5*, 637–650. [[CrossRef](#)] [[PubMed](#)]
21. Wu, Y.; Lee, C.-P.; Mimura, H.; Zhang, X.; Wei, Y. Stable solidification of silica-based ammonium molybdophosphate by allophane: Application to treatment of radioactive cesium in secondary solid wastes generated from Fukushima. *J. Hazard. Mater.* **2018**, *341*, 46–54. [[CrossRef](#)] [[PubMed](#)]
22. Clark, C.J.; McBride, M.B. Chemisorption of Cu(II) and Co(II) on allophane and imogolite. *Clays Clay Miner.* **1984**, *32*, 300–310. [[CrossRef](#)]
23. Jara, A.A.; Violante, A.; Pigna, M.; Mora, M.L. Mutual interactions of sulfate, oxalate, citrate, and phosphate on synthetic and natural allophanes. *Soil Sci. Soc. Am. J.* **2006**, *70*, 337–346. [[CrossRef](#)]
24. Kaufhold, S.; Kaufhold, A.; Jahn, R.; Brito, S.; Dohrmann, R.; Hoffmann, R.; Gliemann, H.; Weidler, P.; Frechen, M. A new massive deposit of allophane raw material from Ecuador. *Clays Clay Miner.* **2009**, *57*, 72–81. [[CrossRef](#)]
25. Wada, S.-I.; Eto, A.; Wada, K. Synthetic allophane and imogolite. *J. Soil Sci.* **1979**, *30*, 347–355. [[CrossRef](#)]
26. Baldermann, A.; Dohrmann, R.; Kaufhold, S.; Nickel, C.; Letofsky-Papst, I.; Dietzel, M. The Fe-Mg-saponite solid solution series—A hydrothermal synthesis study. *Clay Miner.* **2014**, *49*, 391–415. [[CrossRef](#)]
27. Baldermann, A.; Warr, L.N.; Letofsky-Papst, I.; Mavromatis, V. Substantial iron sequestration during green-clay authigenesis in modern deep-sea sediments. *Nat. Geosci.* **2015**, *8*, 885–889. [[CrossRef](#)]
28. Baldermann, A.; Dietzel, M.; Mavromatis, V.; Mittermayr, F.; Warr, L.N.; Wemmer, K. The role of Fe on the formation and diagenesis of interstratified glauconite-smectite and illite-smectite: A case study of Upper Cretaceous shallow-water carbonates. *Chem. Geol.* **2017**, *453*, 21–34. [[CrossRef](#)]
29. Kaufhold, S.; Ufer, K.; Kaufhold, A.; Stucki, J.W.; Anastácio, A.S.; Jahn, R.; Dohrmann, R. Quantification of allophane from Ecuador. *Clays Clay Miner.* **2010**, *58*, 707–716. [[CrossRef](#)]

30. Opiso, E.; Sato, T.; Yoneda, T. Adsorption and co-precipitation behavior of arsenate, chromate, selenate and boric acid with synthetic allophane-like materials. *J. Hazard. Mater.* **2009**, *170*, 79–86. [[CrossRef](#)] [[PubMed](#)]
31. Levard, C.; Doelsch, E.; Basile-Doelsch, I.; Abidin, Z.; Miche, H.; Masion, A.; Rose, J.; Borschneck, D.; Bottero, J.-Y. Structure and distribution of allophanes, imogolite and proto-imogolite in volcanic soils. *Geoderma* **2012**, *183–184*, 100–108. [[CrossRef](#)]
32. Baldermann, A.; Mavromatis, V.; Frick, P.M.; Dietzel, M. Effect of aqueous Si/Mg ratio and pH on the nucleation and growth of sepiolite at 25 °C. *Geochim. Cosmochim. Acta* **2018**, *227*, 211–226. [[CrossRef](#)]
33. Usiyama, T.; Fukushi, K. Predictive model for Pb(II) adsorption on soil minerals (oxides and low-crystalline aluminum silicate) consistent with spectroscopic evidence. *Geochim. Cosmochim. Acta* **2016**, *190*, 134–155. [[CrossRef](#)]
34. Lagergren, S. Zur theorie der sogenannten adsorption gelöster stoffe. *Kungliga Svenska Vetenskapsakademiens* **1898**, *24*, 1–39.
35. Okada, K.; Nishimuta, K.; Kameshima, Y.; Nakajima, A. Effect on uptake of heavy metal ions by phosphate grafting of allophane. *J. Colloid Interface Sci.* **2005**, *286*, 447–454. [[CrossRef](#)] [[PubMed](#)]
36. Kaufhold, A. *Eigenschaften von Allophan aus Ecuador (Santo Domingo de los Colorados) und Anwendungspotential als Rohstoff*; Hallenser Bodenwissenschaftliche Abhandlungen 16: Halle, Germany, 2011; pp. 1–175, ISBN 978-3-86247-172-0. (In German)
37. Chávez, M.L.; de Pablo, L.; García, T.A. Adsorption of Ba²⁺ by Ca-exchange clinoptilolite tuff and montmorillonite clay. *J. Hazard. Mater.* **2010**, *175*, 216–223. [[CrossRef](#)] [[PubMed](#)]
38. Langmuir, I. The adsorption of gases on plane surfaces of glass, mica and platinum. *J. Am. Chem. Soc.* **1918**, *40*, 1361–1403. [[CrossRef](#)]
39. Dubinin, M.M.; Radushkevich, L.V. Equation of the characteristic curve of activated charcoal. *Proc. Acad. Sci. USSR Phys. Chem. Sect.* **1947**, *55*, 331–333.
40. De Gisi, S.; Lofrano, G.; Grassi, M.; Notarnicola, M. Characteristics and adsorption capacities of low-cost sorbents for wastewater treatment: A review. *Sust. Mater. Technol.* **2016**, *9*, 10–40. [[CrossRef](#)]
41. Ghaemi, A.; Torab-Mostaedi, M.; Ghannadi-Maragheh, M. Characterizations of strontium(II) and barium(II) adsorption from aqueous solutions using dolomite powder. *J. Hazard. Mater.* **2011**, *190*, 916–921. [[CrossRef](#)] [[PubMed](#)]
42. Torab-Mostaedi, M.; Ghaemi, A.; Ghassabzadeh, H.; Ghannadi-Maragheh, M. Removal of strontium and barium from aqueous solutions by adsorption onto expanded Perlite. *Can. J. Chem. Eng.* **2011**, *89*, 1247–1254. [[CrossRef](#)]
43. Manohar, D.M.; Noeline, B.F.; Anirudhan, T.S. Adsorption performance of Al-pillared bentonite clay for the removal of cobalt(II) from aqueous phase. *Appl. Clay Sci.* **2006**, *31*, 194–206. [[CrossRef](#)]
44. Bhattacharyya, K.G.; Gupta, S.S. Kaolinite and montmorillonite as adsorbents for Fe(III), Co(II) and Ni(II) in aqueous medium. *Appl. Clay Sci.* **2008**, *41*, 1–9. [[CrossRef](#)]
45. Al-Dwairi, R.A.; Al-Rawajfeh, A.E. Removal of cobalt and nickel from wastewater by using Jordan low-cost zeolite and bentonite. *J. Univ. Chem. Technol. Metall.* **2012**, *47*, 69–76.
46. Mohapatra, M.; Mohapatra, L.; Singh, S.; Anand, S.; Mishra, B.K. A comparative study on Pb(II), Cd(II), Cu(II), Co(II) adsorption from single and binary aqueous solutions on additive assisted nano-structured goethite. *Int. J. Eng. Sci. Technol.* **2010**, *2*, 89–103. [[CrossRef](#)]
47. Bhatnagara, A.; Minocha, A.K.; Sillanpää, M. Adsorptive removal of cobalt from aqueous solution by utilizing lemon peel as biosorbent. *Biochem. Eng. J.* **2010**, *48*, 181–186. [[CrossRef](#)]
48. Chegrouche, S.; Mellah, A.; Barkat, M. Removal of strontium from aqueous solutions by adsorption onto activated carbon: kinetic and thermodynamic studies. *Desalination* **2009**, *235*, 306–318. [[CrossRef](#)]
49. Ahmadpour, A.; Zabihi, M.; Tahmasbi, M.; Rohani Bastami, T. Effect of adsorbents and chemical treatments on the removal of strontium from aqueous solutions. *J. Hazard. Mater.* **2010**, *182*, 552–556. [[CrossRef](#)] [[PubMed](#)]
50. Huang, Y.; Wang, W.; Feng, Q.; Dong, F. Preparation of magnetic clinoptilolite/CoFe₂O₄ composites for removal of Sr²⁺ from aqueous solutions: Kinetic, equilibrium, and thermodynamic studies. *J. Saudi Chem. Soc.* **2017**, *21*, 58–66. [[CrossRef](#)]
51. Elouear, Z.; Bouzid, J.; Boujelben, N.; Feki, M.; Jamoussi, F.; Montiel, A. Heavy metal removal from aqueous solutions by activated phosphate rock. *J. Hazard. Mater.* **2008**, *156*, 412–420. [[CrossRef](#)] [[PubMed](#)]

52. Kyzas, G.Z.; Sifaka, P.I.; Pavlidou, E.G.; Chrissafis, K.J.; Bikiaris, D.N. Synthesis and adsorption application of succinyl-grafted chitosan for the simultaneous removal of zinc and cationic dye from binary hazardous mixtures. *Chem. Eng. J.* **2015**, *259*, 438–448. [[CrossRef](#)]
53. Stojakovic, D.; Hrenovic, J.; Mazaj, M.; Rajic, N. On the zinc sorption by the Serbian natural clinoptilolite and the disinfecting ability and phosphate affinity of the exhausted sorbent. *J. Hazard. Mater.* **2011**, *185*, 408–415. [[CrossRef](#)] [[PubMed](#)]
54. Shahmohammadi-Kalalagh, S.; Babazadeh, H.; Nazemi, A.H.; Manshour, M. Isotherm and kinetic studies on adsorption of Pb, Zn and Cu by kaolinite. *Caspian J. Environ. Sci.* **2011**, *9*, 243–255.
55. Jain, R.; Jordan, N.; Schild, D.; van Hullebusch, E.D.; Weiss, S.; Franzen, C.; Farges, F.; Hübner, R.; Lens, P.N.L. Adsorption of zinc by biogenic elemental selenium nanoparticles. *Chem. Eng. J.* **2015**, *260*, 855–863. [[CrossRef](#)]
56. Richoz, S.; Baldermann, A.; Frauwallner, A.; Harzhauser, M.; Daxner-Höck, G.; Klammer, D.; Piller, W.E. Geochemistry and mineralogy of the Oligo-Miocene sediments of the Valley of Lakes, Mongolia. *Palaeobio. Palaeoenv.* **2017**, *97*, 233–258. [[CrossRef](#)] [[PubMed](#)]
57. Purgstaller, B.; Dietzel, M.; Baldermann, A.; Mavromatis, V. Control of temperature and aqueous Mg^{2+}/Ca^{2+} ratio on the (trans-)formation of ikaite. *Geochim. Cosmochim. Acta* **2017**, *217*, 128–143. [[CrossRef](#)]
58. Mittermayr, F.; Baldermann, A.; Baldermann, C.; Grathoff, G.H.; Klammer, D.; Köhler, S.J.; Leis, A.; Warr, L.N.; Dietzel, M. Environmental controls and reaction pathways of coupled de-dolomitization and thaumasite formation. *Cem. Concr. Res.* **2017**, *95*, 282–293. [[CrossRef](#)]
59. Khan, H. Water Adsorption and Surface Acidity of Nano-Ball Allophane as Affected by Heat Treatment. *J. Environ. Sci. Technol.* **2009**, *2*, 22–30. [[CrossRef](#)]



© 2018 by the authors. Licensee MDPI, Basel, Switzerland. This article is an open access article distributed under the terms and conditions of the Creative Commons Attribution (CC BY) license (<http://creativecommons.org/licenses/by/4.0/>).